

# Laterality and Plasticity of Bone Mineral Density in Vertebral Bodies of Patients with Adolescent Idiopathic Scoliosis

**Takahiro Makino**

Osaka University School of Medicine Graduate School of Medicine: Osaka Daigaku Daigakuin Igakukei  
Kenkyuka Igakubu

**Shota Takenaka**

Osaka University School of Medicine Graduate School of Medicine: Osaka Daigaku Daigakuin Igakukei  
Kenkyuka Igakubu

**Yusuke Sakai**

Osaka University School of Medicine Graduate School of Medicine: Osaka Daigaku Daigakuin Igakukei  
Kenkyuka Igakubu

**Yuya Kanie**

Osaka University School of Medicine Graduate School of Medicine: Osaka Daigaku Daigakuin Igakukei  
Kenkyuka Igakubu

**TAKASHI KAITO** (✉ [takashikaito@gmail.com](mailto:takashikaito@gmail.com))

Osaka University Graduate School of Medicine <https://orcid.org/0000-0003-4882-2997>

---

## Research article

**Keywords:** Adolescent idiopathic scoliosis, Bone mineral density, Plasticity, Laterality, Disc wedging

**Posted Date:** March 19th, 2021

**DOI:** <https://doi.org/10.21203/rs.3.rs-337247/v1>

**License:**  This work is licensed under a Creative Commons Attribution 4.0 International License.

[Read Full License](#)

---

# Abstract

## Background

The asymmetrical distribution of bone mineral density (BMD) in vertebral bodies in adolescent idiopathic scoliosis (AIS) has been reported; however, it is still unknown whether BMD asymmetrical distribution can vary by the mechanical environment around each vertebral body. The purpose of this retrospective study was to investigate changes in the asymmetrical distribution of BMD in each vertebral body up to 1 year after posterior spinal corrective fusion surgery (PSF) in patients with AIS.

## Methods

We analyzed 75 vertebrae within the non-instrumented lumbar spines of 27 female AIS patients (median age, 16 years; interquartile range [IQR], 14–19 years) who underwent PSF. The BMDs of the vertebral bodies were calculated from 1-week and 1-year postoperative quantitative computed tomography scans and a laterality index (LI = BMD of right half of vertebral bodies / BMD of left half of vertebral bodies). The disc wedging angle was measured preoperatively and at 1 year postoperatively from plain radiographs, and the disc wedging angle index (DWAI) was calculated as the sum of the disc wedging angles of the upper and lower discs adjacent to each vertebra.

## Results

The median BMDs of both the right and left halves of each vertebral body significantly decreased from 1 week postoperatively to 1 year postoperatively (right, 228.3 mg/cm<sup>3</sup> hydroxyapatite [IQR, 201.8–251.0 mg/cm<sup>3</sup> hydroxyapatite] to 214.8 mg/cm<sup>3</sup> hydroxyapatite [IQR, 186.9–241.0 mg/cm<sup>3</sup> hydroxyapatite],  $P < 0.001$ ; left, 229.6 mg/cm<sup>3</sup> hydroxyapatite [IQR, 198.7–244.7 mg/cm<sup>3</sup> hydroxyapatite] to 206.3 mg/cm<sup>3</sup> hydroxyapatite [IQR, 188.0–231.9 mg/cm<sup>3</sup> hydroxyapatite],  $P < 0.001$ ). The preoperative median DWAI was 5.0 (IQR, -12.0–13.0) and the 1-week postoperative LI was 1.01 (IQR, 0.95–1.08); these measures were positively correlated ( $\rho = 0.827$ ;  $P < 0.001$ ). The median perioperative change in DWAI was -4 (IQR, -9–10) and the median postoperative change in LI was 0.01 (IQR, -0.02–0.03); these measures were also positively correlated ( $\rho = 0.741$ ;  $P < 0.001$ ).

## Conclusions

The laterality of BMD in each vertebral body in AIS patients was a plastic phenomenon, was deemed a secondary change due to external loading, and was related to the amount of disc wedging.

## Background

Mechanical loading influences the longitudinal growth of the long bones and vertebrae via a phenomenon known as the Hueter–Volkmann Law, which explains that growth is retarded by increased mechanical compression and accelerated by decreased loading [1, 2]. In the sciotic spine, Meir et al.

demonstrated that the loading was greater in the intervertebral disc in the concave annulus than in the convex annulus in patients with scoliosis *in vivo* [3, 4]. Moreover, several authors have indicated that the vicious cycle of asymmetrical loading to the intervertebral disc and vertebral wedge deformities can continue in scoliosis patients [5, 6]. We previously reported the plasticity of vertebral wedge deformities in the scoliotic spine and the differences in plasticity between the regions of the vertebrae (apex or not) or pathologies of scoliosis [7, 8].

Despite discussions of morphometric asymmetry and plasticity of vertebral bodies in adolescent idiopathic scoliosis (AIS) [7–11], little attention has been paid to either the asymmetrical distribution or plasticity of bone mineral density (BMD) in each vertebral body in AIS. One reason is that the generally used dual-energy x-ray absorptiometry (DEXA) scans for the measurement of BMD are not reliable in the presence of axial rotation of vertebral bodies in AIS [12]. Furthermore, the DEXA cannot analyze the distribution of the BMD within a given vertebral body.

It has been suggested that patients with AIS have abnormal systemic bone metabolism, and there is confirmation of asymmetric expression of a susceptibility gene for AIS, which regulates osteogenic differentiation of human mesenchymal stem cells, in the vertebral bodies of these patients [13–17]. Recent image processing technology development enables us to analyze 3-dimensional *in vivo* measurements of radiographical parameters. Using quantitative computed tomography (qCT), Adam and Askin reported the asymmetrical distribution of BMD in vertebral bodies in AIS [18]. However, it is still unknown whether BMD asymmetrical distribution can vary by the mechanical environment around each vertebral body according to the Hueter–Volkmann Law. We hypothesized that if the asymmetrical distribution of the BMD is inherent in vertebral bodies and is a characteristic of the systemic bone metabolism in AIS, it remains unchanged even after an increase or decrease in asymmetrical loading by corrective surgery. Thus, the purpose of this study was to reveal the changes in BMD asymmetrical distribution in each vertebral body up to 1 year after posterior corrective fusion surgery in patients with AIS.

## Methods

This retrospective review of a radiological database of patients with AIS who underwent posterior corrective surgery was approved by the Research Ethics Committee of Osaka University Hospital (no. 15098-5). The research ethics committee of our institution waived receipt of written informed consent, because all clinical and radiographic interventions in the study followed routine assessments and the study was retrospective. Instead, the patients were allowed to opt out of the study based on the research information published on our institution's website.

### ***Patients and surgical procedure***

We enrolled all consecutive female AIS patients who had undergone posterior corrective fusion between February 2017 and August 2019 and whose age at the time of surgery was between 10 and 20 years ( $n = 30$ ). Three patients who underwent computed tomography (CT) scans without a hydroxyapatite phantom

were excluded. Thus, 27 patients were included in this study. The median age at the time of surgery was 16 years (interquartile range [IQR], 14–19 years).

All surgeries were performed through the conventional posterior spinal approach under general anesthesia and neuromonitoring. After exposure of posterior spinal bony elements, pedicle screws were inserted into as many pedicles as possible. If the pedicle screws could not be inserted due to anatomical problems, hooks or sublaminar tapings were substituted. A Grade 1 osteotomy (resection of inferior facet) was performed in each fusion segment and a Grade 2 osteotomy (resection of both inferior and superior facets and ligamentum flavum) was performed in each rigid segment where segmental flexibility was not confirmed in preoperative traction and side-bending plain radiographs. After instrumentation, we corrected coronal and sagittal alignments and directly rotated vertebrae to correct 3-dimensional deformities. The autologous local bone graft and hydroxyapatite were transplanted on the decorticated lamina and articular surfaces. Neither iliac bone grafts nor bone morphogenic proteins were used in any of the cases. The patients were banned from participating in sports activities for 1 year after surgery.

### ***Patients' demographic data***

From medical charts, we obtained each patient's age at the time of surgery, preoperative body mass index, and levels of lowest instrumented vertebrae.

### ***Radiographic assessments***

Each patient's type of scoliosis was classified according to the Lenke classification on the basis of preoperative, full-length, standing, posteroanterior, and lateral radiographs [19]. Preoperative and 1-year postoperative Cobb angles of the main thoracic (MT) and thoracolumbar/lumbar (TL/L) curves and preoperative Risser grades were measured on a flat-panel monitor at our hospital using built-in imaging software (SYNAPSE 5; FUJIFILM Medical Systems, USA, Inc., Lexington, MA).

The disc wedging angle, which was defined as the angle between the upper and lower endplates adjacent to the disc (left open, +), was measured in every disc below a lowest instrumented vertebra (Fig. 1). In addition, a disc wedging angle index (DWAI), which was defined as the sum of the upper and lower disc wedging angles adjacent to a vertebra, was calculated in every vertebra within the non-instrumented lumbar spine (Fig. 1). The perioperative change in DWAI ( $\Delta$ DWAI = 1-year postoperative value – preoperative value) was also calculated (Fig. 1).

### ***CT assessments***

The patients underwent routine CT scans about 1 week and 1 year postoperatively for the purpose of detecting mispositioning of instrumentation or confirmation of bone union. CT images were acquired using 1 of 2 scanners (Discovery CT750 HD, GE Healthcare Japan, Tokyo, Japan, or Aquilion ONE, Toshiba Medical Systems Corporation, Tochigi, Japan). The scans used a slice thickness of 0.625 mm with the Discovery CT750 HD and of 0.5 mm with the Aquilion ONE; a tube voltage of 120 kVp; a matrix of 512 × 512; and a standard algorithm. The tube current was maintained by an automatic exposure

control system. Each CT scan imaged together a standardized spine phantom consisting of 5 rods containing 0, 50, 100, 150, and 200 mg/cm<sup>3</sup> hydroxyapatite (HA) (B-MAS 200; Kyoto Kagaku Co., Ltd., Kyoto, Japan). Multiplanar reconstruction was performed by our institution's built-in 3-dimensional imaging software (Synapse Vincent; FUJIFILM Medical Systems, USA, Inc., Lexington, MA). From the 1-week and 1-year postoperative CT scans, each vertebra within the non-instrumented lumbar spine was superimposed automatically by the built-in application of the Synapse Vincent (Fig. 2); then, spherical regions of interest (ROIs) for measurements of Hounsfield Unit (HU) values were set in each vertebral body, excluding the cortical margin on the superimposed 3-dimensional images so that the ROIs should be in the same area on both scans. The centers of the spherical ROIs were set in each vertebral body as follows (Fig. 3):

1. At the center of each vertebral body (ROI representing the whole of each vertebral body);
2. At the center of the right half of each vertebral body (ROI representing the right half of each vertebral body); and
3. At the center of the left half of the vertebral body (ROI representing the left half of each vertebral body).

The BMD (mg/cm<sup>3</sup> HA) of each ROI was calculated by substituting the HU values into the linear regression equation obtained from the measured values of the phantom in each scan. The laterality index (LI) of BMD in each vertebral body was calculated by the following equation:

$$LI = (\text{BMD of right half of the vertebral body}) / (\text{BMD of left half of the vertebral body})$$

The postoperative change in the LI ( $\Delta LI = 1\text{-year postoperative value} - 1\text{-week postoperative value}$ ) was also calculated.

### ***Statistical analysis***

The statistical analysis was performed using IBM SPSS Statistics Version 25 (IBM, Armonk, NY, USA). The Wilcoxon signed rank test was used to compare Cobb angles of preoperative and 1-year postoperative MT and TL/L curves and 1-week postoperative and 1-year postoperative BMDs. Spearman's rank correlation coefficient was used for a correlation analysis. Differences were considered statistically significant at  $P$  values  $< 0.05$ .

## **Results**

The patients' demographic data, preoperative Risser grades, curve profiles, and levels of lowest instrumented vertebrae are shown in Table 1. We analyzed a total of 75 vertebrae within non-instrumented lumbar spines.

Table 1  
Demographic data and scoliosis profile.

<b>Age at time of surgery, years</b>	<b>16 (14–19)</b>
Lenke classification, number of patients	
Type 1	9
Type 2	4
Type 3	2
Type 4	1
Type 5	8
Type 6	3
Preoperative body mass index, kg/m <sup>2</sup>	19.4 (17.6–21.7)
Preoperative Risser grade, number of patients	
1	1
2	0
3	0
4	13
5	13
Lowest instrumented vertebra, number of patients	
T12	3
L1	4
L2	4
L3	16

Values are expressed as medians (interquartile ranges).

The median preoperative and 1-year postoperative Cobb angles were 47.0° (IQR, 35.5–57.0°) and 18.6° (IQR, 15.0–24.8°), respectively, in the MT curve and 43.0° (IQR, 36.6–48.0°) and 15.0° (IQR, 12.0–19.0°), respectively, in the TL/L curve. The Cobb angles of both the MT and TL/L curves were corrected significantly after surgery ( $P < 0.001$ ).

The overall BMD and the BMDs of both the right and left halves of each vertebral body significantly decreased from 1 week postoperatively to 1 year postoperatively (both  $P$  values  $< 0.001$ ; Table 2).

Table 2

Bone mineral density ( $\text{mg/cm}^3$  hydroxyapatite) of vertebral bodies in non-instrumented lumbar spine.

	1 week postoperatively	1 year postoperatively	P value
Whole	230.9 (203.1–246.6)	211.3 (188.0–236.1)	< 0.001
Right half	228.3 (201.8–251.0)	214.8 (186.9–241.0)	< 0.001
Left half	229.6 (198.7–244.7)	206.3 (188.0–231.9)	< 0.001

Values are expressed as medians (interquartile ranges).

The median preoperative DWAI was 5.0 (IQR, –12.0 to 13.0) and the 1-week postoperative LI was 1.01 (IQR, 0.95–1.08); these measures were significantly, positively correlated ( $p = 0.827$ ;  $P < 0.001$ ; Fig. 4). The median  $\Delta$ DWAI was –4 (IQR, –9 to 10) and the median  $\Delta$ LI was 0.01 (IQR, –0.02 to 0.03); these measures were significantly, positively correlated ( $p = 0.741$ ;  $P < 0.001$ ; Fig. 5).

## Discussion

This study showed that BMDs of vertebral bodies in non-instrumented lumbar spines decreased from immediately after surgery to 1 year after surgery. In addition to a decrease in the overall BMD of vertebral bodies, the BMDs also decreased in both the right and left halves of the vertebral bodies postoperatively; also, there were positive correlations between the preoperative DWAI and 1-week postoperative LI and between the perioperative change in DWAI and postoperative change in LI. These facts imply that the laterality of BMD in each vertebral body was changeable and disc wedging was significant factor for the laterality of BMD.

A limitation of this study is that we only analyzed the BMDs of those vertebral bodies in the non-instrumented lumbar spine, because metal artifacts prevented postoperative BMD measurements in the instrumented thoracic spine. However, we confirmed spontaneous correction of scoliosis in our patients even in the non-instrumented lumbar spine, which we believe reflects the altered effects of external loading due to correction of scoliosis on BMD of vertebral bodies in AIS.

The other limitation is the lack of data on long-term postoperative BMD changes, since frequent CT scans can increase radiation exposure for patients and are not ethically acceptable. However, to the best of our knowledge, this is the first report to use qCT *in vivo* to reveal postoperative BMD changes in vertebral bodies in AIS patients.

The BMD of each vertebral body decreased from 1 week postoperatively to 1 year postoperatively. Previous reviews showed that physical activity during growth leads to increased BMD and bone mineral content [20, 21]. Kontulainen et al. revealed that adolescent girls who underwent a 9-month training

intervention of weekly step aerobics and jumping had a 4.9% greater increase in bone mineral content at the lumbar spine compared to those who did not do the training intervention [22]. Thus, we speculate that the overall decrease in the BMD of the vertebral bodies resulted from prohibiting participation in sports activities for 1 year after surgery.

A previous report indicated that the asymmetrical distribution of BMD in vertebral bodies in AIS, which was most obvious around the apex of the scoliotic curve, was an adaptive response to asymmetrical loading to the vertebral bodies [18]. Our present study also revealed the asymmetrical distribution of BMD in each vertebral body. The positive correlation between the preoperative DWAI and 1-week postoperative LI in our study indicates that the BMD of the concave side was larger than that of the convex side in each vertebral body, and the asymmetrical distribution of BMD in each vertebral body became obvious from the increasing disc wedging angle adjacent to the vertebral body. Moreover, the positive correlation between the perioperative change in DWAI and the postoperative change in LI also indicates that the BMD became relatively higher on the side where the intervertebral discs were “compressed” due to surgery than on the side where the intervertebral discs were “stretched.” These results show that external loading via intervertebral discs alters not only the morphometries of vertebral bodies but also the distribution of BMD in each vertebral body according to the Hueter–Volkmann Law, and indicates that this asymmetrical distribution of BMD in AIS is a plastic phenomenon.

It has been reported that high bone turnover or low BMD can be associated with curve severity or progression of AIS, and poor BMD can be an etiopathogenesis in AIS [13–15, 17, 23, 24]. Furthermore, Xu et al. observed asymmetric expression of GPR126, which is considered a susceptibility gene for AIS and plays an important role for ossification of the developing spine [25], in the vertebral bodies of AIS patients [16]. Their study revealed that overexpression of GPR126 delayed osteogenic differentiation of human mesenchymal stem cells, and transcripts of GPR126 were expressed significantly more in the convex side than in the concave side of vertebral bodies [16]. These genetical facts could result in the laterality of BMD in each vertebral body, although it is still unknown whether the laterality of BMD is associated with the etiology of AIS or curve progression. Our hypothesis was that the asymmetrical distribution of BMD in each vertebral body in AIS patients, if it was the sequence of the inherent abnormal bone metabolism, would remain unchanged even after an increase or decrease in asymmetrical loading from corrective surgery. However, from our results, the laterality of BMD in each vertebral body was plastic and was related to the degree of wedging deformity of the intervertebral discs. Therefore, even if an abnormal bone metabolism can be an etiology of developing AIS, we speculate that the laterality of BMD in each vertebra is not the primary change but the secondary change, due to asymmetrical loading to each vertebral body.

## Conclusions

We evaluated the BMD of each vertebral body in the non-instrumented lumbar spine of patients after receiving posterior corrective fusion surgery for AIS, and found that the BMDs decreased until 1 year postoperatively. The asymmetrical distribution of BMD was more obvious in those vertebrae with more

disc wedging, and the BMD of the concave side was larger than that of the convex side. Furthermore, this laterality of BMD was a plastic phenomenon, and the amount of change in the disc wedging angle was positively related to the amount of change in laterality of BMD in each vertebral body. Therefore, the laterality of BMD in each vertebral body is considered to be a secondary change due to external loading rather than a primary etiopathogenesis of AIS.

## Abbreviations

BMD, bone mineral density; AIS, adolescent idiopathic scoliosis; PSF, posterior spinal fusion; IQR, interquartile range; LI, laterality index; DWAI, disc wedging angle index; DEXA, dual-energy x-ray absorptiometry; qCT, quantitative computed tomography; CT, computed tomography; MT, main thoracic; TL/L, thoracolumbar/lumbar; HA, hydroxyapatite; ROI, region of interest; HU, Hounsfield Unit.

## Declarations

### ***Ethics approval and consent to participate***

All procedures performed were in accordance with the 1964 Declaration of Helsinki. This research has been approved by the Research Ethics Committee of Osaka University Hospital (no. 15098-5). The research protocol was approved and publicized by the authors' affiliated institution, and the patients were given the right to opt out of the study.

### ***Consent for publication***

Not applicable.

### ***Availability of data and materials***

The datasets generated during the current study are available from the corresponding author on reasonable request.

### ***Competing interest***

The Author(s) declare(s) that there is no conflict of interest with respect to the research, authorship, and/or publication of this article.

### ***Funding***

This work was supported by JSPS KAKENHI Grant Number18K16657.

### ***Authors' contributions***

TM designed the study. All authors contributed to data collection. TM drafted the manuscript. TK contributed to supervision of this study. All authors read and approved the final manuscript.

## Acknowledgements

None.

## References

1. Stokes IA. Mechanical effects on skeletal growth. *J Musculoskel Neuronal Interact*. 2002;2(3):277–80.
2. D'Andrea C, Alfraihat A, Singh A, Anari JB, Cahill PJ, Schaer T, Snyder BD, Elliott D, Balasubramanian S. **Part 1. Review and Meta-Analysis of Studies on Modulation of Longitudinal Bone Growth and Growth Plate Activity: A Macro-Scale Perspective.** *Journal of orthopaedic research: official publication of the Orthopaedic Research Society* 2020.
3. Meir AR, Fairbank JC, Jones DA, McNally DS, Urban JP. High pressures and asymmetrical stresses in the scoliotic disc in the absence of muscle loading. *Scoliosis*. 2007;2:4.
4. Meir A, McNally DS, Fairbank JC, Jones D, Urban JP: **The internal pressure and stress environment of the scoliotic intervertebral disc – a review.** *Proceedings of the Institution of Mechanical Engineers Part H, Journal of engineering in medicine* 2008, **222**(2):209–219.
5. Stokes IA, Spence H, Aronsson DD, Kilmer N. Mechanical modulation of vertebral body growth. Implications for scoliosis progression. *Spine (Phila Pa 1976)*. 1996;21(10):1162–7.
6. Sarwark J, Aubin CE. Growth considerations of the immature spine. *J Bone Joint Surg Am*. 2007;89(Suppl 1):8–13.
7. Makino T, Kaito T, Sakai Y, Takenaka S, Sugamoto K, Yoshikawa H. Plasticity of vertebral wedge deformities in skeletally immature patients with adolescent idiopathic scoliosis after posterior corrective surgery. *BMC Musculoskelet Disord*. 2016;17(1):424.
8. Makino T, Sakai Y, Kashii M, Takenaka S, Sugamoto K, Yoshikawa H, Kaito T. Differences in vertebral morphology around the apical vertebrae between neuromuscular scoliosis and idiopathic scoliosis in skeletally immature patients: a three-dimensional morphometric analysis. *BMC Musculoskelet Disord*. 2017;18(1):459.
9. Schlosser TP, van Stralen M, Brink RC, Chu WC, Lam TP, Vincken KL, Castelein RM, Cheng JC. Three-dimensional characterization of torsion and asymmetry of the intervertebral discs versus vertebral bodies in adolescent idiopathic scoliosis. *Spine (Phila Pa 1976)*. 2014;39(19):E1159–66.
10. Begon M, Scherrer SA, Coillard C, Rivard CH, Allard P. Three-dimensional vertebral wedging and pelvic asymmetries in the early stages of adolescent idiopathic scoliosis. *Spine J*. 2015;15(3):477–86.
11. Brink RC, Schlosser TPC, Colo D, Vincken KL, van Stralen M, Hui SCN, Chu WCW, Cheng JCY, Castelein RM. Asymmetry of the Vertebral Body and Pedicles in the True Transverse Plane in Adolescent Idiopathic Scoliosis: A CT-Based Study. *Spine deformity*. 2017;5(1):37–45.
12. Cheng JC, Sher HL, Guo X, Hung VW, Cheung AY. The effect of vertebral rotation of the lumbar spine on dual energy X-ray absorptiometry measurements: observational study. *Hong Kong medical journal = Xianggang yi xue za zhi*. 2001;7(3):241–5.

13. Lee WT, Cheung CS, Tse YK, Guo X, Qin L, Lam TP, Ng BK, Cheng JC: **Association of osteopenia with curve severity in adolescent idiopathic scoliosis: a study of 919 girls.** *Osteoporosis international: a journal established as result of cooperation between the European Foundation for Osteoporosis and the National Osteoporosis Foundation of the USA* 2005, **16**(12):1924–1932.
14. Yu WS, Chan KY, Yu FW, Yeung HY, Ng BK, Lee KM, Lam TP, Cheng JC. Abnormal bone quality versus low bone mineral density in adolescent idiopathic scoliosis: a case-control study with in vivo high-resolution peripheral quantitative computed tomography. *Spine J.* 2013;13(11):1493–9.
15. Yip BHK, Yu FWP, Wang Z, Hung VWY, Lam TP, Ng BKW, Zhu F, Cheng JCY. Prognostic Value of Bone Mineral Density on Curve Progression: A Longitudinal Cohort Study of 513 Girls with Adolescent Idiopathic Scoliosis. *Scientific reports.* 2016;6:39220.
16. Xu E, Lin T, Jiang H, Ji Z, Shao W, Meng Y, Gao R, Zhou X. Asymmetric expression of GPR126 in the convex/concave side of the spine is associated with spinal skeletal malformation in adolescent idiopathic scoliosis population. *Eur Spine J.* 2019;28(9):1977–86.
17. Diarbakerli E, Savvides P, Wihlborg A, Abbott A, Bergström I, Gerdhem P. Bone health in adolescents with idiopathic scoliosis. *The bone joint journal.* 2020;102-b(2):268–72.
18. Adam CJ, Askin GN. Lateral bone density variations in the scoliotic spine. *Bone.* 2009;45(4):799–807.
19. Lenke LG, Betz RR, Harms J, Bridwell KH, Clements DH, Lowe TG, Blanke K: **Adolescent idiopathic scoliosis: a new classification to determine extent of spinal arthrodesis.** *J Bone Joint Surg Am* 2001, **83-a**(8):1169–1181.
20. Specker B, Thieb NW, Sudhagnani RG. Does Exercise Influence Pediatric Bone? A Systematic Review. *Clin Orthop Relat Res.* 2015;473(11):3658–72.
21. Troy KL, Mancuso ME, Butler TA, Johnson JE. **Exercise Early and Often: Effects of Physical Activity and Exercise on Women's Bone Health.** *International journal of environmental research and public health* 2018, **15**(5).
22. Kontulainen SA, Kannus PA, Pasanen ME, Sievänen HT, Heinonen AO, Oja P, Vuori I. Does previous participation in high-impact training result in residual bone gain in growing girls? One year follow-up of a 9-month jumping intervention. *Int J Sports Med.* 2002;23(8):575–81.
23. Li X, Hung VWY, Yu FWP, Hung ALH, Ng BKW, Cheng JCY, Lam TP, Yip BHK. Persistent low-normal bone mineral density in adolescent idiopathic scoliosis with different curve severity: A longitudinal study from presentation to beyond skeletal maturity and peak bone mass. *Bone.* 2020;133:115217.
24. Zhang J, Wang Y, Cheng KL, Cheuk K, Lam TP, Hung ALH, Cheng JCY, Qiu Y, Müller R, Christen P, et al. Association of higher bone turnover with risk of curve progression in adolescent idiopathic scoliosis. *Bone.* 2021;143:115655.
25. Kou I, Takahashi Y, Johnson TA, Takahashi A, Guo L, Dai J, Qiu X, Sharma S, Takimoto A, Ogura Y, et al. Genetic variants in GPR126 are associated with adolescent idiopathic scoliosis. *Nat Genet.* 2013;45(6):676–9.

## Figures

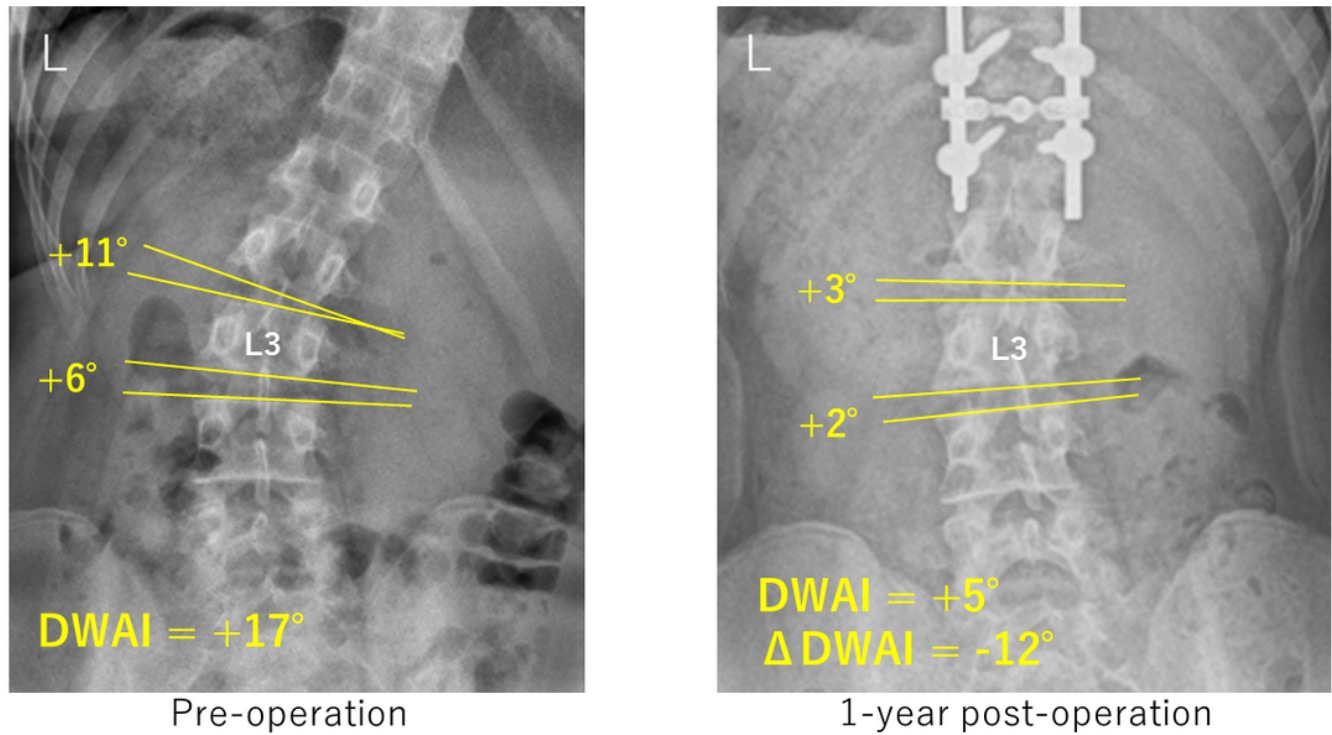


**Figure 1**

An example measurement of a disc wedging angle index (DWAI) of L3. The perioperative change in DWAI ( $\Delta$ DWAI = 1-year postoperative value–preoperative value) was calculated.

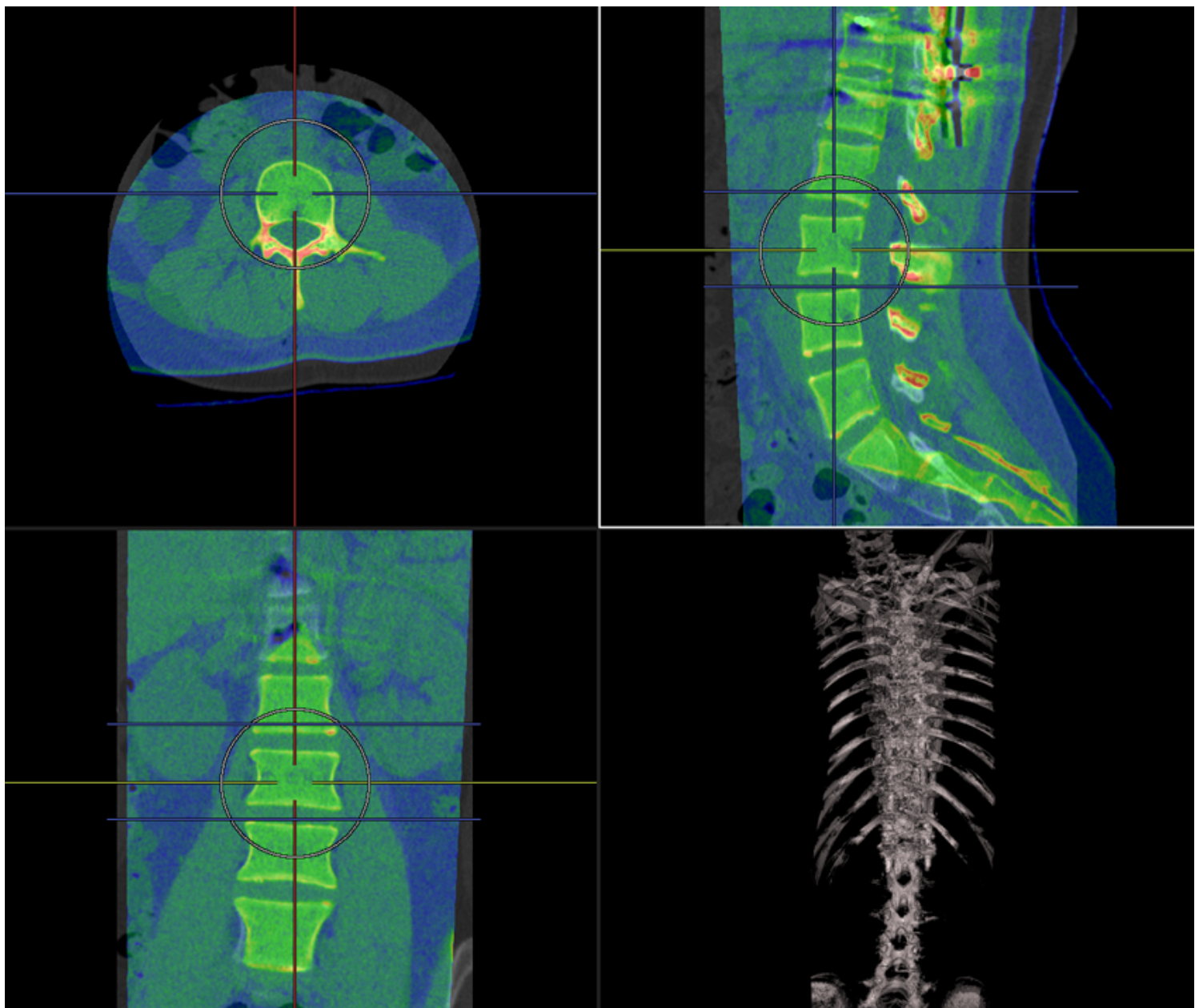


**Figure 2**

An example of an L3 vertebra in which 1-week postoperative (color scale) and 1-year postoperative (gray scale) computed tomography scans were automatically superimposed by the built-in application.

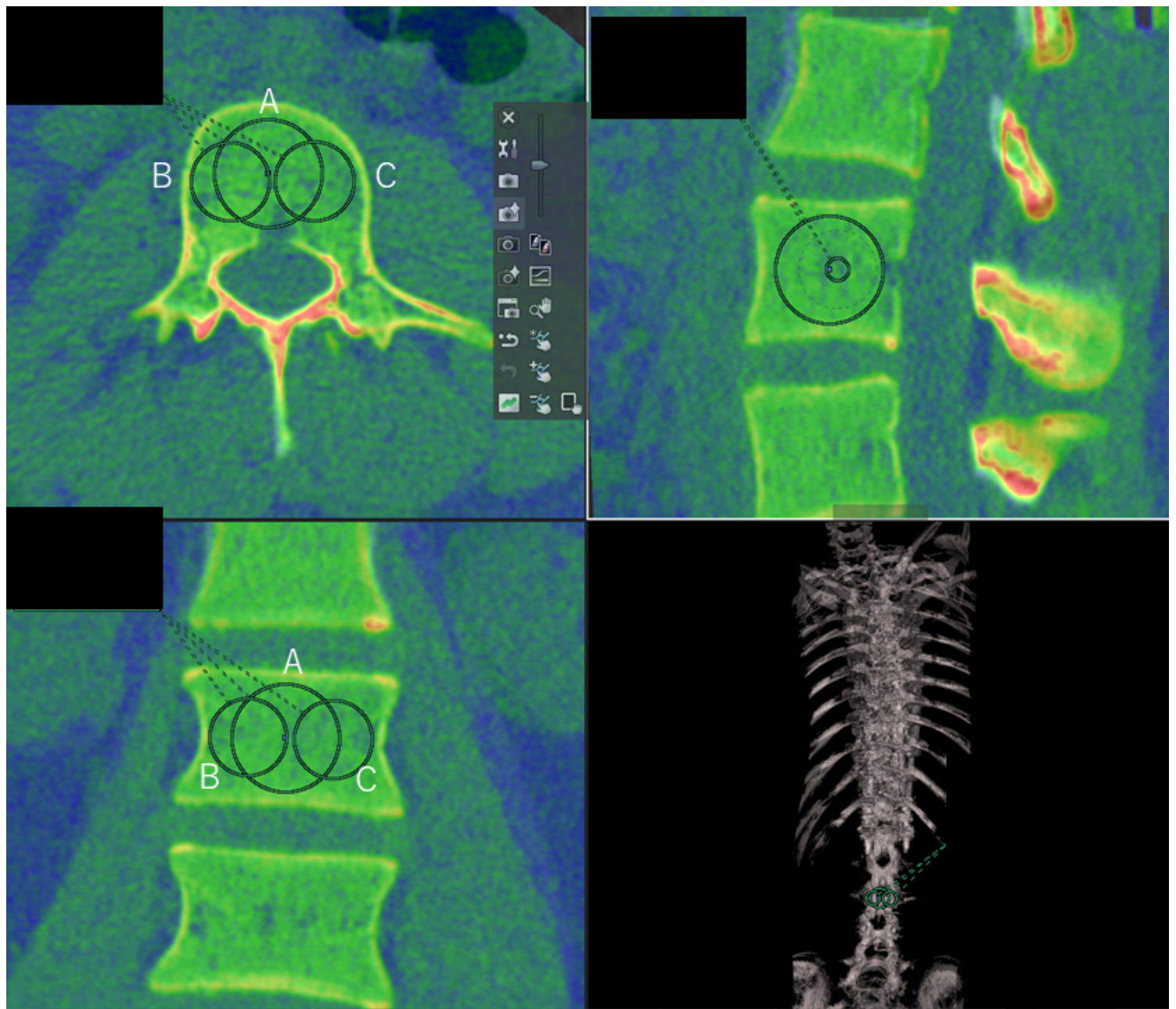


**Figure 3**

An example of setting spherical regions of interest (ROIs) for measurements of Hounsfield Unit values in the L3 vertebral body on the superimposed 3-dimensional images. A indicates the ROI for the whole vertebral body; B shows the ROI for the right half of the vertebral body; and C shows the ROI for the left half of the vertebral body.

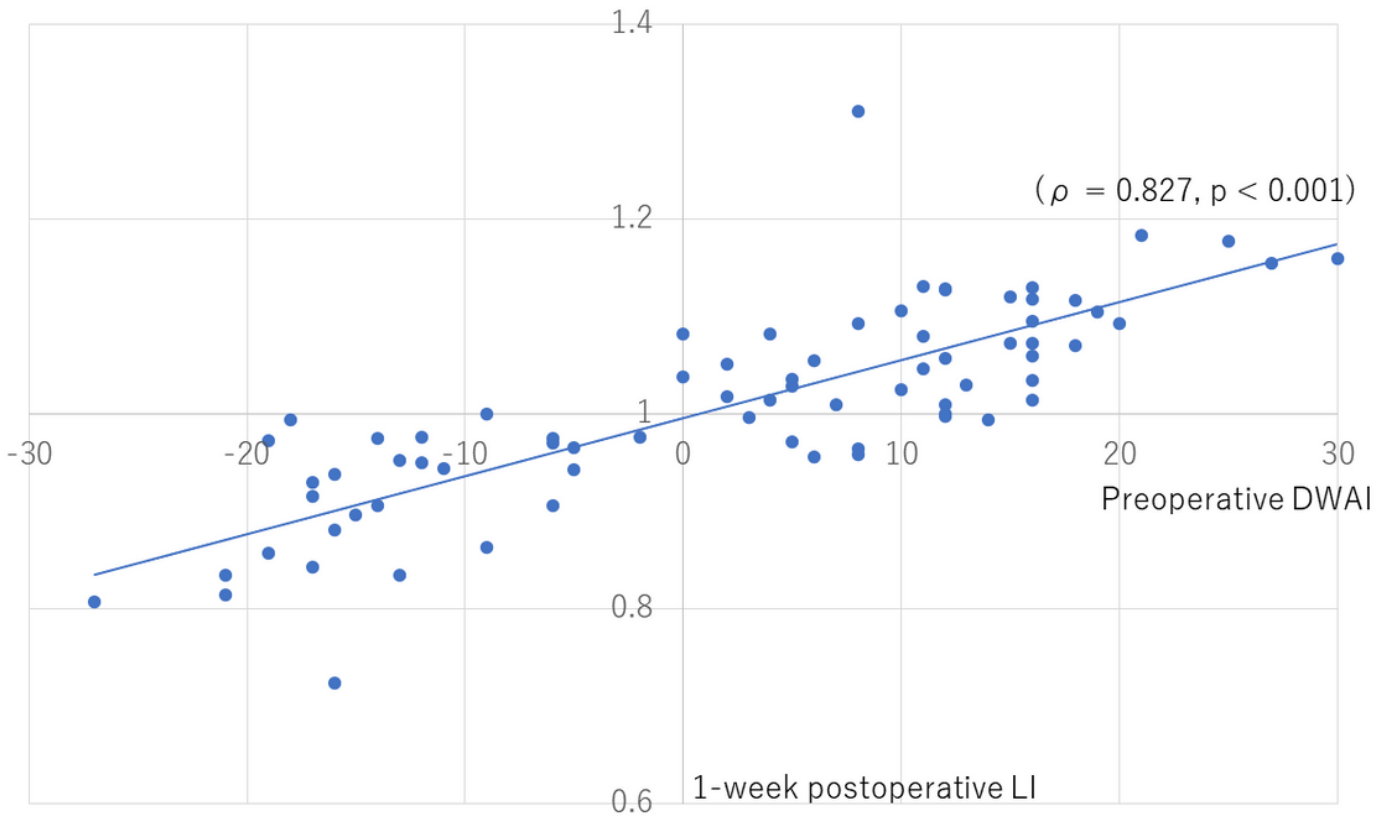


**Figure 4**

A scatter plot representing the correlation between the preoperative disc wedging angle index (DWAI) and the 1-week postoperative laterality index (LI), which were significantly, positively correlated ( $\rho = 0.827$ ;  $P < 0.001$ ).

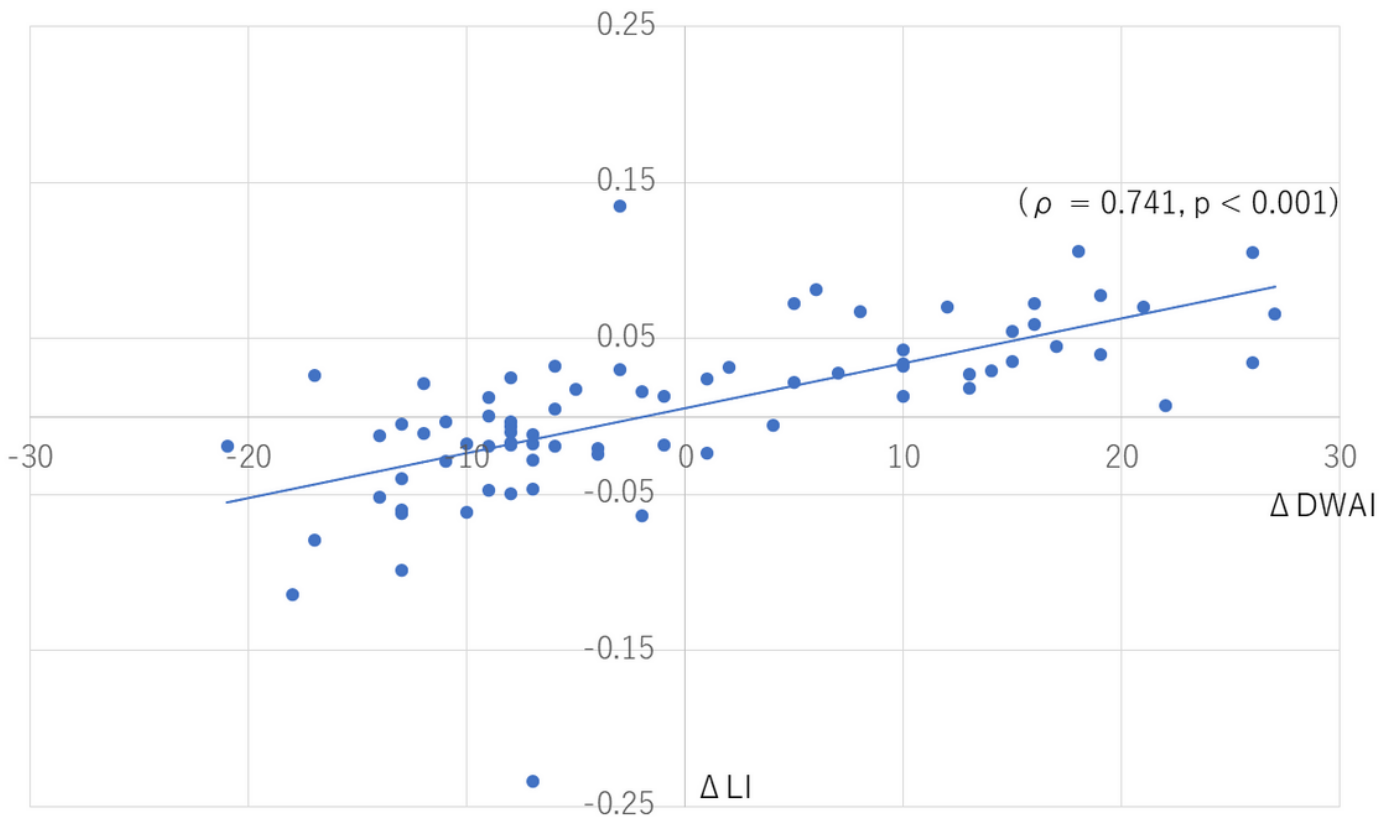


**Figure 5**

A scatter plot representing the correlation between perioperative changes in the disc wedging angle index ( $\Delta$ DWAI = 1-year postoperative value – preoperative value) and postoperative changes in the laterality index ( $\Delta$ LI = 1-year postoperative value–1-week postoperative value), which were significantly, positively correlated ( $\rho = 0.741$ ;  $P < 0.001$ ).